The Journal of Experimental Biology 212, 1559-1567
Published by The Company of Biologists 2009
doi:10.1242/jeb.027383

Cloning and functional expression of the first eukaryotic Na^+–tryptophan symporter, AgNAT6

Ella A. Meleshkevitch[1], Marvin Robinson[2], Lyudmila B. Popova[2,3], Melissa M. Miller[2], William R. Harvey[2] and Dmitri Y. Boudko[1,*]

[1]Department of Physiology and Biophysics, Rosalind Franklin University of Medicine and Science, 3333 Green Bay Road, North Chicago, IL 60064, USA, [2]Whitney Laboratory for Marine Bioscience, University of Florida, St Augustine, FL 32080, USA and [3]A. N. Belozersky Institute, Moscow State University, Moscow, 119899, Russia

*Author for correspondence (e-mail: dmitri.boudko@rosalindfranklin.edu)

Accepted 10 March 2009

SUMMARY

The nutrient amino acid transporter (NAT) subfamily of the neurotransmitter sodium symporter family (NSS, also known as the solute carrier family 6, SLC6) represents transport mechanisms with putative synergistic roles in the absorption of essential and conditionally essential neutral amino acids. It includes a large paralogous expansion of insect-specific genes, with seven genes from the genome of the malaria mosquito, *Anopheles gambiae.* One of the *An. gambiae* NATs, AgNAT8, was cloned, functionally expressed and characterized in *X. laevis* oocytes as a cation-coupled symporter of aromatic amino acids, preferably L-phenylalanine, L-tyrosine and L-DOPA. To explore an evolutionary trend of NAT-SLC6 phenotypes, we have cloned and characterized AgNAT6, which represents a counterpart of AgNAT8 descending from a recent gene duplication (53.1% pairwise sequence identity). In contrast to AgNAT8, which preferably mediates the absorption of phenol-branched substrates, AgNAT6 mediates the absorption of indole-branched substrates with highest apparent affinity to tryptophan ($K_{0.5}^{Trp}$=1.3 μmol l^{-1} *vs* $K_{0.5}^{Phe}$=430 μmol l^{-1}) and [2 or 1 Na^+ or K^+]:[aromatic substrate] stoichiometry. AgNAT6 is highly transcribed in absorptive and secretory regions of the alimentary canal and specific neuronal structures, including the neuropile of ventral ganglia and sensory afferents. The alignment of AgNATs and $LeuT_{Aa}$, a bacterial NAT with a resolved 3D structure, reveals three amino acid differences in the substrate-binding pocket that may be responsible for the indole- *vs* phenol-branch selectivity of AgNAT6 *vs* AgNAT8. The identification of transporters with a narrow selectivity for essential amino acids suggests that basal expansions in the SLC6 family involved duplication and retention of NATs, improving the absorption and distribution of under-represented essential amino acids and related metabolites. The identified physiological and expression profiles suggest unique roles of AgNAT6 in the active absorption of indole-branched substrates that are used in the synthesis of the neurotransmitter serotonin as well as the key circadian hormone and potent free-radical scavenger melatonin.

Key words: NAT, AgNAT8, synergy.

INTRODUCTION

The aromatic amino acids – phenylalanine, tyrosine and tryptophan – are critical for animal health and development. They serve as the metabolic precursors of proteins, signaling peptides, monoamine neurotransmitters and hormones. However, animal metabolism tends to be deficient in essential aromatic amino acids that are not synthesized *de novo*. The exception is tyrosine, which can be produced in animal cells from the essential precursor phenylalanine. In addition, aromatic amino acids comprise the most under-represented group of ecological nutrient chains [on average phenylalanine accounts for 3.00%, tyrosine for 3.06% and tryptophan for 1.02% of the amino acid residues in proteins (Brooks et al., 2002)]. In meeting metabolic demands, metazoan cells actively absorb aromatic amino acids despite low membrane permeability and unfavorable concentration gradients (Chakrabarti, 1994; Chakrabarti and Deamer, 1994). However, there is a serious knowledge gap regarding the molecular mechanisms of absorption. For example, no presently known metazoan transporter is able to transport adequate amounts of tryptophan due to insufficient selectivity, spatial distribution or energy-coupling mechanisms. In contrast after a highly selective tryptophan transporter was found in the prokaryotic neurotransmitter sodium symporter family (NSS, also known as solute carrier family 6, SLC6 by HUGO nomenclature). The *tnaT* gene encodes a unique Na^+-dependent mechanism with strong tryptophan selectivity. It has been cloned from *Symbiobacterium thermophilum* (Androutsellis-Theotokis et al., 2003), a microorganism whose growth depends on commensalism and whose genome includes several transporters for peptides and amino acids (Ueda et al., 2004), but only one SLC6 member. The tnaT transporters mediate Na^+ gradient-coupled uptake of tryptophan and act in synergy with other members of the *tnaT* operon of *S. thermophilum* that grow in nutrient-enriched media (Ueda et al., 2004). The SLC6 family expands dramatically in Metazoa (~20 members per genome in mammals and insects compared with 0–4 members per genome in prokaryotes) with segregation into two large subfamilies: neurotransmitter transporters (NTTs) and nutrient amino acid transporters (NATs) (Boudko et al., 2005b). NTTs absorb two signaling amino acids, Gly and GABA, and the essential aromatic amino acid precursors of the signaling monoamines: dopamine, serotonin, norepinephrine (noradrenaline) and octopamine. All characterized NATs mediate [Na^+ or K^+]:[neutral amino acid] symport. The metazoan NATs are functional counterparts and evolutionary progeny of prokaryotic SLC6 members such as tnaT.

Ironically, *S. thermophilum*, a compost bacterium, possesses a single SNF member per genome that mediates the absorption of energy-rich tryptophan for catabolic fuel, but no active tryptophan transporter has been identified in metazoan organisms, even though it is their most essential nutrient.

Previously, we characterized the first of the seven NAT-SLC6 members in the *Anopheles gambiae* genome, AgNAT8 (Meleshkevitch et al., 2006). It mediates Na^+ (or K^+)-coupled symport of L-phenylalanine, L-tyrosine and 3,4-dihydroxy-L-phenylalanine (L-DOPA). In the absence of these substrates, AgNAT8 can absorb L-tryptophan and 5-hydroxytryptophan (5-HTP); however, it cannot acquire the indole-branched substrates in the presence of physiological concentrations of phenyl-branched substrates. Now, we have cloned and characterized AgNAT6, a phylogenetically close relative of AgNAT8. It absorbs tryptophan and, with less efficiency, other aromatic substrates. The identified indole- and phenol-branch-specific AgNATs have surprisingly little variation in their substrate-binding pockets, exhibiting only three amino acid differences that are likely to be responsible for their unique selectivity profiles. The AgNAT6 expression pattern correlates with tissues that are involved in nutrient absorption and neuronal functions.

MATERIALS AND METHODS

Cloning and heterologous expression

AgNAT6 was cloned from a cDNA collection of *An. gambiae* larval midgut into pGEM-T and pXOON vectors as described elsewhere (Meleshkevitch et al., 2006). Exact primers with or without *Bam*HI (5′-cgG GAT CCc gAT GGC GAC CAG TAA TCC GGC CTT T-3′) and *Eco*RI (5′-cgG AAT TCcg TCA ACT GAA CAC GTT GTC GAA CAT-3′) flanking sequences (underlined) were used to obtain PCR products which were inserted into the *Bam*HI/*Eco*RI-digested expression vector pXOON (Jespersen et al., 2002) or the pGEM-T cloning vector, respectively. cRNA for oocyte injections was obtained by *in vitro* transcription of *Pme*I-linearized AgNAT6-pXOON plasmids using mMessage mMachine®, a high-yield, capped RNA transcription kit (Ambion, Austin, TX, USA). Surgically isolated and collagenase-treated stage V–VI *Xenopus laevis* oocytes (Nasco, Fort Atkinson, WI, USA) were injected with ~40 ng of AgNAT6 cRNA and incubated for 2–6 days at 17°C in sterile N98-oocyte medium (Boudko et al., 2005a). AgNAT6-injected oocytes were analyzed in a small volume perfusion chamber using 2-electrode voltage clamp techniques identical to those used to characterize AgNAT8 (Meleshkevitch et al., 2006).

Bioinformatics

AgNAT6 sequence fragments were assembled using SeqManII (DNASTAR, Madison, WI, USA). Homologous sequences were derived from non-redundant protein databases (NCBI). The phylogenetic analysis included 63 SLC6 members from selected dipteran genomes plus a few reference sequences of cloned NAT-SLC6 members. The protein alignments were generated using ClustalX (Thompson et al., 1997) and visualized using GeneDoc software (Nicholas et al., 1977). A phylogenetic tree was constructed using Mega 4 software (Tamura et al., 2007). Fine-tuning of the alignment was performed manually by considering sequence and 3D structure alignments of selected NATs with LeuT (PDB ID 2a65) (Yamashita et al., 2005). Homology modeling was performed by satisfaction of spatial restraints (Sali and Blundell, 1993) using Modeler (Marti-Renom et al., 2000).

Quantitative real-time polymerase chain reaction assay (qPCR)

RNA isolation, cDNA synthesis and qPCR analysis were performed as described previously (Meleshkevitch et al., 2006). Primers were designed with the following sequences: 5′-GGC AAC ACC AGT CGA ACC A-3′ and 5′-GCT GCA CCT TGT GGA TGT TCT-3′. Expression of AgNAT6 in each tissue was normalized to that found in whole larvae, which was set to a value of one. Data represent three averaged replicates of three independent experiments. Excel software (Microsoft Inc., Redmond, WA, USA) was used to collect and analyze data and SigmaPlot 10 (Systat Software, Inc., San Jose, CA, USA) was used to generate final graphs.

Isotope uptake assay

Uptake assays were performed 4 days after RNA injection on oocytes using a previously described protocol (Meleshkevitch et al., 2006). Briefly, distilled water (DW)- and AgNAT6 RNA-injected oocytes were exposed in a 100 mmol l^{-1} NaCl solution supplemented with 10 μCi ml^{-1} L-[5-^{3}H]tryptophan or L-[2,3,4,5,6-^{3}H]phenylalanine (specific activity 25 and 125 μCi mmol l^{-1}, respectively, Amersham Biosciences, Piscataway, NJ, USA), brought to a final concentration of 1 mmol l^{-1} with unlabeled tryptophan or phenylalanine. Uptake was terminated after 10 min by washing oocytes with a cold 100 mmol l^{-1} choline chloride solution. Pairs of oocytes were placed in scintillation vials with 200 μl of 10% SDS; 4 ml of scintillation fluid was added, and the radioactivity was counted using a Beckman-Coulter LS 6500 scintillation counter (Beckman-Coulter, Inc., Fullerton, CA, USA). The quantity and ratio of substrate uptake were calculated as described earlier (Meleshkevitch et al., 2006). The measured ratio values were normalized *vs* the value for radiolabeled L-tryptophan uptake in AgNAT6 transcript-injected oocytes.

Whole-mount *in situ* hybridization

Anopheles gambiae larvae (G3 strain) were hatched from eggs supplied by MR4 (The Malaria Research and Reference Reagents Resource Center, Atlanta, GA, USA) and raised as described earlier (Okech et al., 2008b). A purified pGEM-T AgNAT6 plasmid was linearized with *Nco*I or *Not*I restriction enzymes to obtain full-length, run-off transcripts using SP6 and T7 promoters for anti-sense and sense probes, respectively. DIG-labeled probes were transcribed *in vitro* using a DIG RNA labeling kit (Roche Diagnostics, Mannheim, Germany). Fourth instar *An. gambiae* larvae were immobilized in ice-cold phosphate-buffered saline (PBS, Fisher Scientific, Itasca, IL, USA) opened by a lateral incision, and fixed in 4% paraformaldehyde/PBS overnight. Preparations were dehydrated/rehydrated by passing through a PBS/methanol gradient set (100% PBS–3:1–1:1–1:3–100% methanol, then in reverse order), 10 min for each mixture, pre-treated with proteinase K/detergent solution (0.1% Tween-20 in PBS supplemented with 10 μg ml^{-1} proteinase K) for 30–40 min. The preparation was pre-hybridized for 6–8 h at 50°C in hybridization solution (50% formamide, 5 mmol l^{-1} EDTA, 5× SSC, 1× Denhardt's solution, 0.1% Tween-20, 0.5 mg ml^{-1} yeast tRNA), then hybridized by incubation with approximately 1 μg of DIG-labeled RNA probe per ml of hybridization solution at 50°C overnight. The hybridized preparations were labeled with alkaline phosphatase-conjugated, anti-DIG antibodies according to the manufacturer's protocol. Hybridization patterns were visualized in a NBT/BCIP alkaline buffer solution (Boehringer Mannheim, Inc., GmbH, Mannheim, Germany). Labeled preparations were embedded in 3:1 glycerol:PBS on glass slides and photographed using an Olympus SZX 12 stereo microscope (Olympus America, Center

Valley, PA, USA) and Pixera CCD camera (Pixera Corp., Los Gatos, CA, USA).

Data analysis

Values depicted in graphs represent the mean ± s.d. from at least three different experiments using at least three different oocytes. The electrical current amplitudes were normalized relative to a maximum current in each data set. Kinetic profiles and constants were derived by fitting normalized data sets with a three-parameter sigmoidal Hill function $y=ax^b/(c^b+x^b)$; where: $a=y\text{max}$, the derived maximum current; $b=\eta$, the order of the transport process; $c=x_{50\%}$; $(x, y)=K_{0.5,[S]}$, the substrate concentration at 50% of the transport velocity.

RESULTS

AgNAT6 was cloned from a midgut cDNA collection of 4th instar mosquito larvae (GenBank CDS AJ626713 and PID CAF25029). It has a 1953 bp ORF encoding a 650 amino acid-long protein with an estimated molecular mass of 71.5 kDa and pI of 7.31. It is the closest phylogenetic relative to the earlier characterized Na^+–phenylalanine, phenyl-branched substrate symporter AgNAT8 (Fig. 1; pairwise similarity 52.9%, identical sites 343, 51.7%) and a newly characterized member of the NATs subfamily of the SLC6 family. The AgNAT6 and AgNAT8 genes result from the most recent duplication in the AgNAT-SLC6 cluster (Fig. 2). They are the first upstream and the last downstream genes, respectively, of a seven-gene NAT cluster that is mapped on the positive strand of the 3L chromosome between 12.09 and 12.16 Mb positions (Meleshkevitch et al., 2006), based on the genome annotation (Holt et al., 2002).

AgNAT6 has a typical SLC6 structure with 12 transmembrane domains and intracellular C and N termini (Fig. 1). Twelve coordinating organic substrate residues are identifiable based on the sequence-structure alignment of AgNAT6, AeAAT1 (Boudko et al., 2005a), AgNAT8 (Meleshkevitch et al., 2006) and TnaT (Androutsellis-Theotokis et al., 2003) with crystallized $LeuT_{Aa}$ (Yamashita et al., 2005) (Fig. 1; Table 1). The substrate-interacting moieties comprise a surprisingly conserved pattern, with nine absolutely conserved sites between AgNAT6 and AgNAT8 (Table 1). Three different amino acids in transmembrane domains 1, 6 and 8 could be responsible for the tryptophan selectivity of AgNAT6. Specifically they include: L91, because this site is different from a corresponding M95 site in AgNAT8; T333, which is different from AgNAT8 S339 and identical to TnaT T234, and G437 which is unique to AgNAT6 (d, i and u indicate corresponding sites in Table 1). These three positions correspond to N21, S356 and A358 of $LeuT_{Aa}$. All three substitutions aid in the reduction of the side-chain volume and corresponding increases in the substrate-binding envelope volume, which correlates with a capacity to accept larger sized indole- *vs* phenol-branched substrates (Fig. 3A, inset).

The expression of all seven AgNATs, nine AeNATs and six DmNATs was confirmed by molecular cloning from specific cDNA collections (all 22 clone sequences are available in the NCBI database, see Fig. 1 for NCBI accession numbers), but presently only two AgNATs have been characterized by heterologous expression; previously, AgNAT8 (Meleshkevitch et al., 2006) and, now, AgNAT6. The application of aromatic amino acids produced a barely detectable current in naive and DW-injected *X. laevis* oocytes (<5 nA at 1 mmol l^{-1} concentration of aromatic substrate in ND98 at –50 mV holding transmembrane potential, Hp; data not shown).

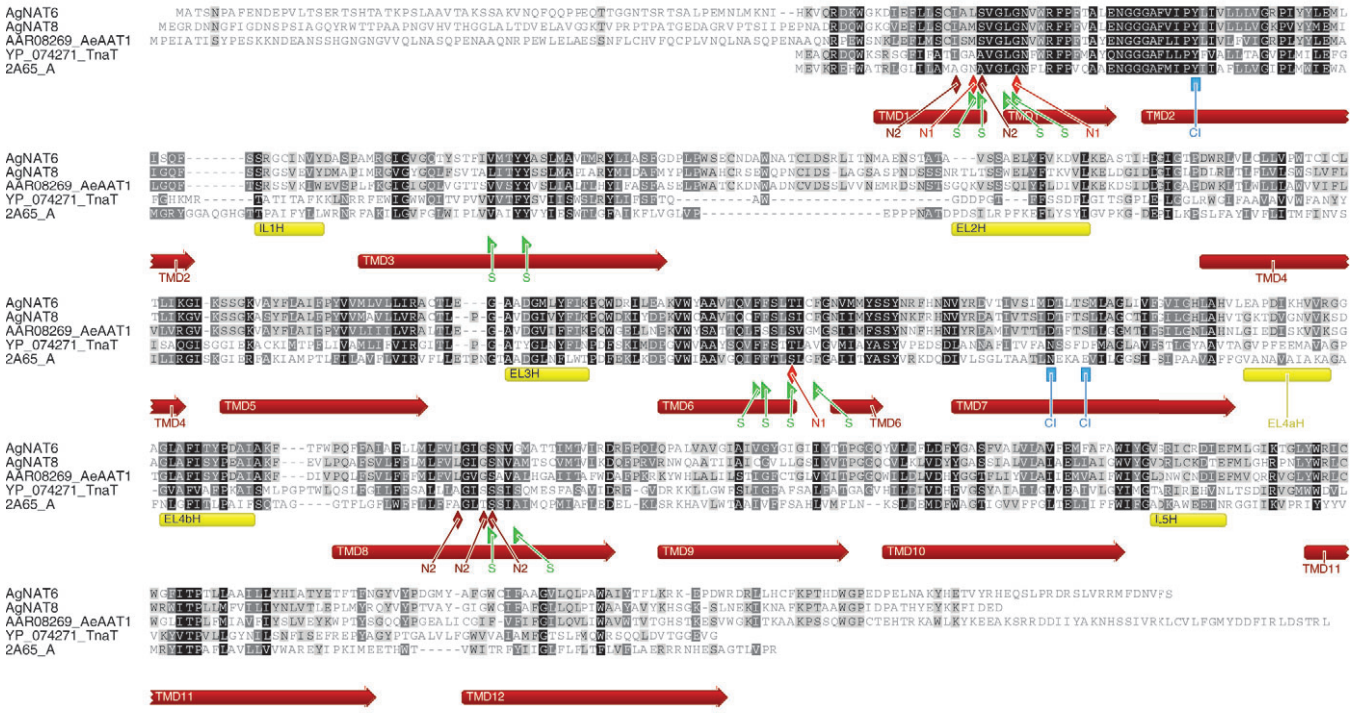

Fig. 1. Alignment of AgNAT6 with selected insect and bacterial nutrient amino acid transporters (NATs). Transmembrane domains (TMD1–12) and conserved structural features including substrate interaction sites were identified after alignment of AgNAT6 with selected insect and prokaryotic NATs including $LeuT_{Aa}$ sequence (this figure), which is supported by structural alignment, and substrate docking (not shown). The alignment was generated by Geneious Pro 4.5 software (Biomatters, Auckland, New Zealand) with a minor manual improvement. Increasing background intensity indicates an increase in sequence similarity. Green triangles indicate substrate-binding sites, red and brown rhombuses are first and second Na^+ interacting sites, purple squares represent Cl^--binding sites. Dark red arrows are transmembrane helices; yellow bars are sub-membrane (EL, extracellular loop; IL, intracellular loop) helices.

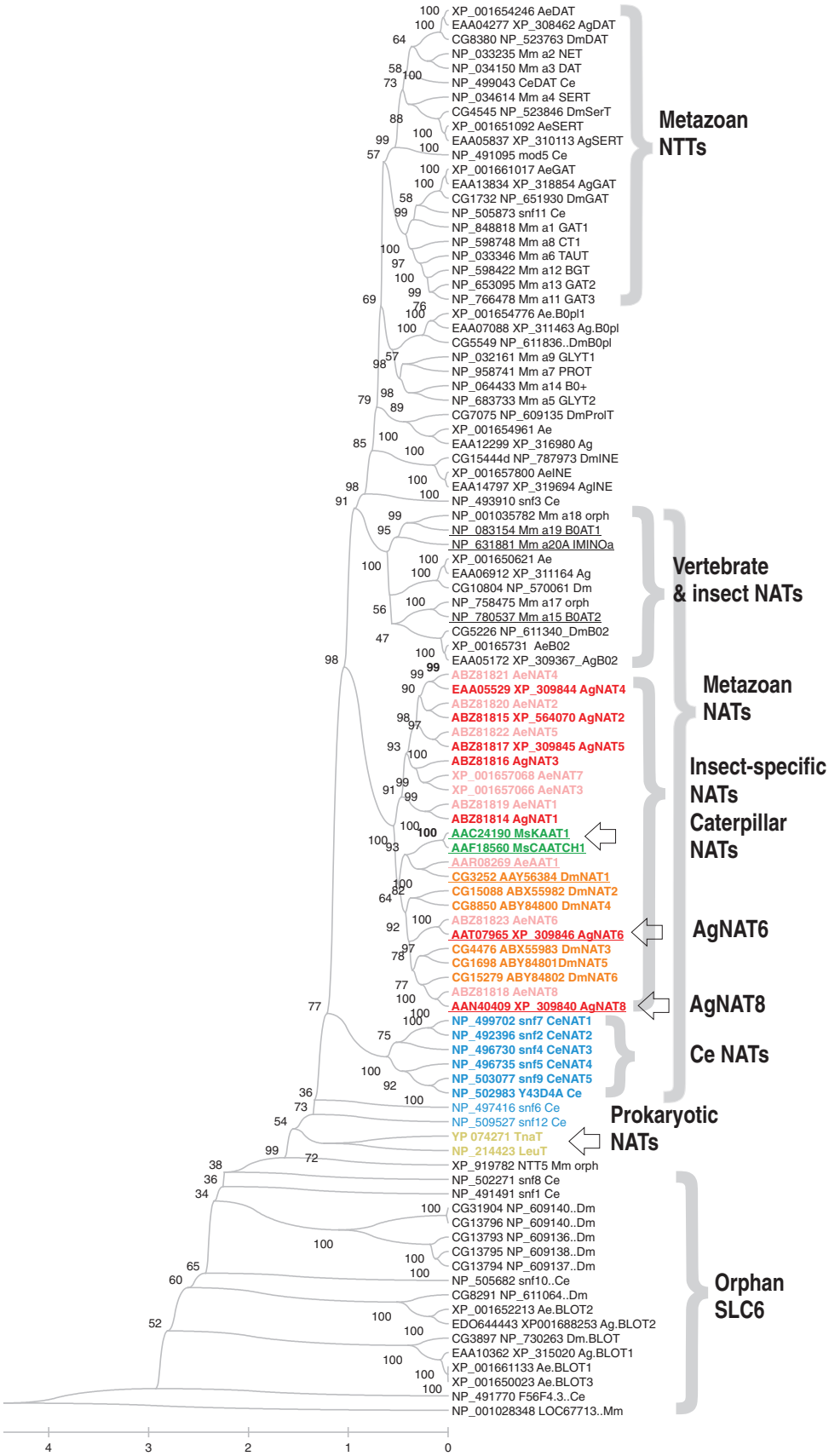

Fig. 2. Phylogenetic position of AgNAT6 in the solute carrier family 6 (SLC6) tree. The tree includes 98 SLC6 members from seven completed genomes including one mammalian, three dipteran insect, one nematode and two prokaryotic genomes; two characterized lepidopteran NAT sequences were also added. The evolutionary history was inferred using the UPGMA method (Sneath and Sokal, 1973). The optimal tree with a sum of branch length=63.23 is shown. The percentage of replicate trees in which the associated taxa clustered together in the bootstrap test (2000 replicates) is shown next to the branches (Felsenstein, 1985). The tree is drawn to scale, with branch lengths in the same units as those of the evolutionary distances used to infer the phylogenetic tree. The evolutionary distances were computed using the Poisson correction method (Zuckerkandl and Pauling, 1965) and are in units of the number of amino acid substitutions per site. The rate variation among sites was modeled with a gamma distribution (shape parameter=1). All positions containing alignment gaps and missing data were eliminated only in pairwise sequence comparisons (pairwise deletion option). There were a total of 566 positions in the final dataset. Phylogenetic analyses were conducted in MEGA4 (Tamura et al., 2007). Lines show NCBI accession numbers followed by arbitrary definitions of obvious orthologs and cloned transporters (shown in bold). Abbreviations: Ae, *Aedes* aegypti; Ag, *Anopheles gambiae*; Ce, *Caenorhabditis elegance*; Dm, *Drosophila melanogaster*; Mm, *Mus musculus*; Ms, *Manduca sexta*; NTTs, neurotransmitter transporters. Discussed transporters are underlined. Invertebrate NATs are depicted by different font colors.

Table 1. Alignment of substrate-binding envelopes of selected prokaryotic and eukaryotic NATs

TMD no.	11111-333-666666-888	Phenotype
AgNAT6	LS-LG-V-Y-FF-T-F-S-G	Trp specific
AgNAT8	MS-LG-L-Y-FF-S-F-S-A	Phe specific
AeAAT1	MS-LG-V-Y-FS-S-M-S-A	Phe broad
TnaT	AA-LG-V-Y-FF-T-V-S-S	Trp specific
LeuT	NA-LG-V-Y-FF-S-F-S-A	Leu broad
Sites:	dc-cc-c-c-cc-i-c-c-u	

NAT, nutrient amino acid transporter; Ae, *Aedes aegypti*; Ag, *Anopheles gambiae*; TMD, transmembrane domain.

Substrate-interacting sites: c, conserved in AgNAT6 and AgNAT8; d, different in AgNAT6 and AgNAT8; i, identical in Trp-specific eukaryotic and prokaryotic transporters; u, unique in AgNAT6.

AgNAT6 expression increased a background leak current from 7±5 nA to 82±24 nA, N>100 at –30 mV Hp) and mediated large aromatic amino acid-induced currents of 20–150 nA (Fig. 3A). In contrast to phenylalanine-preferring AgNAT8, AgNAT6 responded with notably larger currents upon tryptophan and 5-HTP application (Fig. 3B), suggesting a higher transport velocity for indole- than phenol-branched substrates. Among Phe-derived metabolites only Trp (addition of a hydroxyl group to the end of the 6-carbon aromatic ring with corresponding increase in molecular volume) produced currents that were similar to the indole-branch substrate-induced currents (Fig. 3A). Replacing Na^+ with Li^+ or K^+ abolished tryptophan-induced currents at –30 mV Hp (Fig. 3D). However, the extended current–voltage (I–V) graph revealed that AgNAT6 can generate large substrate-coupled K^+ currents at transmembrane voltages more negative than –40 mV (Fig. 3E). Isotope-uptake experiments confirmed AgNAT6-coupled organic substrate uptake with notably higher uptake ratios for isotope-labeled tryptophan than for phenylalanine (Fig. 3F).

The AgNAT6 mechanism has saturable kinetics (Fig. 4A). Tryptophan has a remarkably higher apparent affinity than all other tested substrates (K_{50}^{Trp}=1.3 µmol l^{-1} compared with $K_{0.5}^{5\text{-HTP}}$=270<$K_{0.5}^{Tyr}$<$K_{0.5}^{Phe}$<$K_{0.5}^{DOPA}$<$K_{0.5}^{Leu}$=890 µmol l^{-1}). The orders of the organic substrate translocation reaction (Hill constant η) determined at 98 mmol l^{-1} Na^+ concentrations were all similar and approached 1 (Fig. 4B).

AgNAT6 tested at two different concentrations of tryptophan showed little increase in K_{50}^{Na+} at 3 mmol l^{-1} Trp *vs* 0.3 mmol l^{-1} Trp (Fig. 4C). Unexpectedly, we have identified a capacity of AgNAT6 to exhibit Hill coefficients of 2 and 1 Na^+ for tryptophan translocations at 0.3 and 3 mmol l^{-1} concentrations, respectively

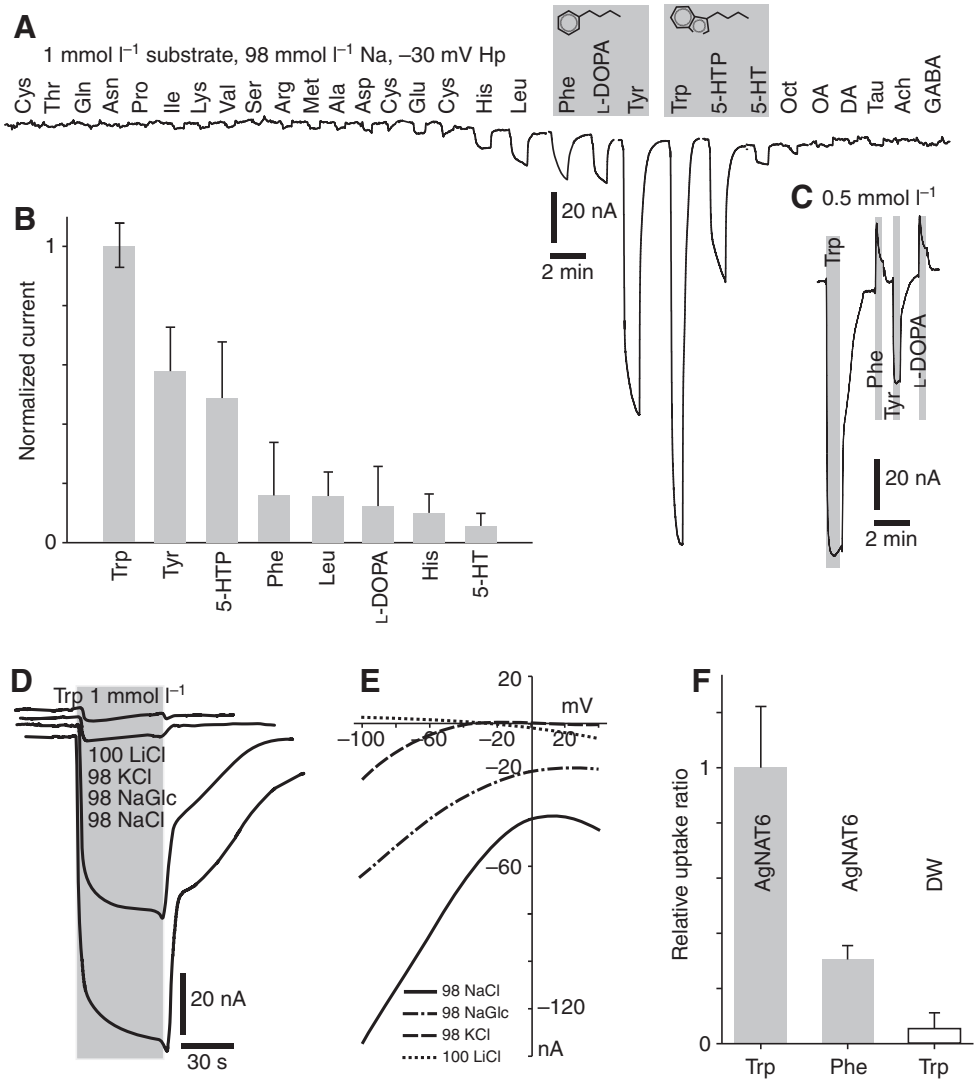

Fig. 3. Electrochemical properties of AgNAT6 mechanism expressed in *Xenopus laevis* oocytes. (A) An example of substrate-induced currents obtained from a representative oocyte. All substrates were superfused at 1 mmol l^{-1} concentrations in 98 mmol l^{-1} NaCl media at –30 mV holding transmembrane voltage potential. (B) Normalized substrate-induced currents (bars are means ± s.d. for N>3 experiments and oocytes). (C) Unusual positive responses, which often but not always were observed after application of L-Phe and L-DOPA at 6–8 days after cRNA injection. (D) Ion dependency of a Trp-induced current. Millimolar concentrations of the major salt component of perfusion solutions are shown in the order of current traces above. (E) I–V plots of AgNAT6 interactions with Trp at specific compositions of inorganic ions; plots represent current–voltage relationships following subtraction of the Trp-independent current component. I–V plots relating to perfusion solutions containing different major salts are depicted by different line styles (see key). (F) Relative uptake ratios calculated after a 10 min exposure of the AgNAT6-injected (filled bars) and distilled water (DW)-injected (open bar) oocytes to specified isotope-labeled substrate (bars are normalized mean uptake ratio ±s.d., N=3).

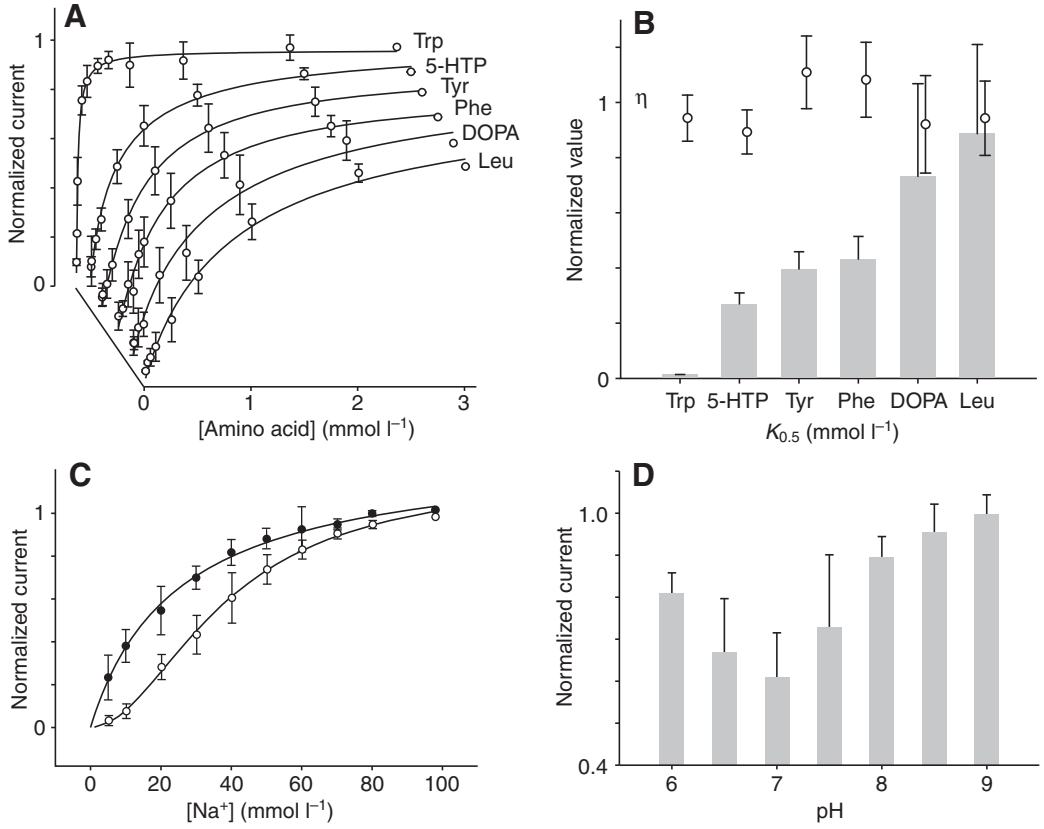

Fig. 4. Kinetic properties and pH dependency of AgNAT6. AgNAT6-mediated currents as a function of concentration of selected organic substrates (A) and sodium ions at 0.3 and 3 mmol l^{-1} concentrations of tryptophan (C). Curves are non-linear regression of the data calculated from the Hill equation: $f=ax^{\eta}/(K_{0.5}{}^{\eta}+x^{\eta})$; 3 mmol l^{-1} Trp (filled circles), η=0.98±0.14, $K_{0.5}$=25.27±6.38 and 0.3 mmol l^{-1} Trp (open circles), η=1.90±0.21, $K_{0.5}$=38.46±3.47 in C. (B) Estimated affinity constants (bars are means ± s.d., N>3) and Hill constants (circles are means ± s.d., N>3) for selected organic substrates. (D) pH dependency of AgNAT6 (circles are means ± s.d., N>3).

(Fig. 4C). This 'slip' may suggest a switch of the preferred transport stoichiometry in the AgNAT6 mechanism: 1 Na^+:1 amino acid at high concentrations of organic substrates and 2 Na^+:1 amino acid at low concentrations of organic substrates. AgNAT6 showed non-linear pH dependency with relatively high transport turnover at moderately acidic (pH 6) and strongly alkaline (pH 8–9) *vs* neutral (pH 7) external solutions.

In situ hybridization of the larval alimentary canal with an AgNAT6 antisense probe revealed a relatively high accumulation of AgNAT6 transcript in the heart, gastric caeca and posterior midgut (Fig. 5A). Weaker but detectable labeling was present in the anterior midgut (Fig. 5A). Strong *in situ* hybridization signals were detected in the neuronal plexus of the larval head associated with chemo-, visual- and mechano-sensory modalities and in the neuropile of the ventral nerve cord (Fig. 5B,C). A strong signal was detected in a few individual neurons upon low resolution imaging of whole-mount preparations (images not shown). A very strong signal was also detected in the 2nd and 3rd instar larval alimentary canal, especially when young larvae were exposed to limited nutrient conditions (Fig. 5D). qPCR confirmed a ubiquitous expression of AgNAT6 with very strong tissue-specific and developmental stage-specific variations of AgNAT6 transcript quantities (Fig. 5E).

DISCUSSION

Several transporters which are thought to translocate aromatic amino acids *via* the plasma membrane of metazoan cells have been characterized previously (Table 2). However, the molecular identity of an active mechanism for absorbing tryptophan remained enigmatic. Here we report the molecular cloning and characterization of AgNAT6, the first metazoan transporter with definite roles in the absorption and systemic redistribution of tryptophan and related indole-branched substrates.

AgNAT6 is a new member of the NAT-SLC6 subfamily (Fig. 1). All currently characterized NATs encode transporters with similar electrochemical mechanisms utilizing the most ubiquitous monovalent cation (primarily Na^+) electrochemical gradient to symport (co-transport) neutral amino acids. The NATs population includes broad substrate spectrum, neutral amino acid transporters, which were identified in mammals (Broer et al., 2004) and insects [see figure 1s, B^0AT1 and DmNAT1, in Miller et al. (Miller et al., 2008)]. In insects the NAT subfamily has an additional expansion, which is absent in mammals. This expansion includes seven genes in *An. gambiae* (Fig. 2). One of these genes, AgNAT8, was recently characterized as a Na^+-dependent, voltage-driven (Harvey et al., 2009) mechanism that is adapted to transport phenylalanine and its related metabolites (Meleshkevitch et al., 2006). The present characterization of its closest phylogenetic relative, AgNAT6, reveals a different mechanism, specializing in the active absorption of tryptophan and its related metabolites. AgNAT6 and AgNAT8 are expressed in similar loci and may act in synergy to optimize the absorption of indole- or phenyl-branched substrates, respectively (Okech et al., 2008b). The aromatic AgNATs result from earlier gene fission in the NAT population of *An. gambiae* that may correspond with adaptations of mosquito larvae for development in habitats with a low level of essential nutrients. The identified properties of AgNAT6 fit with our previous hypothesis that NATs undergo rapid gene duplication which drives the specialization of individual transporters and adaptive plasticity of integrated NAT functions (Boudko et al., 2005a).

AgNAT6, like all other characterized NATs, is a rectifying, normally irreversible, transporter (Fig. 3E). Both aromatic AgNATs use Na^+ electromotive forces; however, they could utilize K^+ electromotive forces with appropriate inward directions (Fig. 3E). In this respect they represent a transitional phenotype between Na^+-

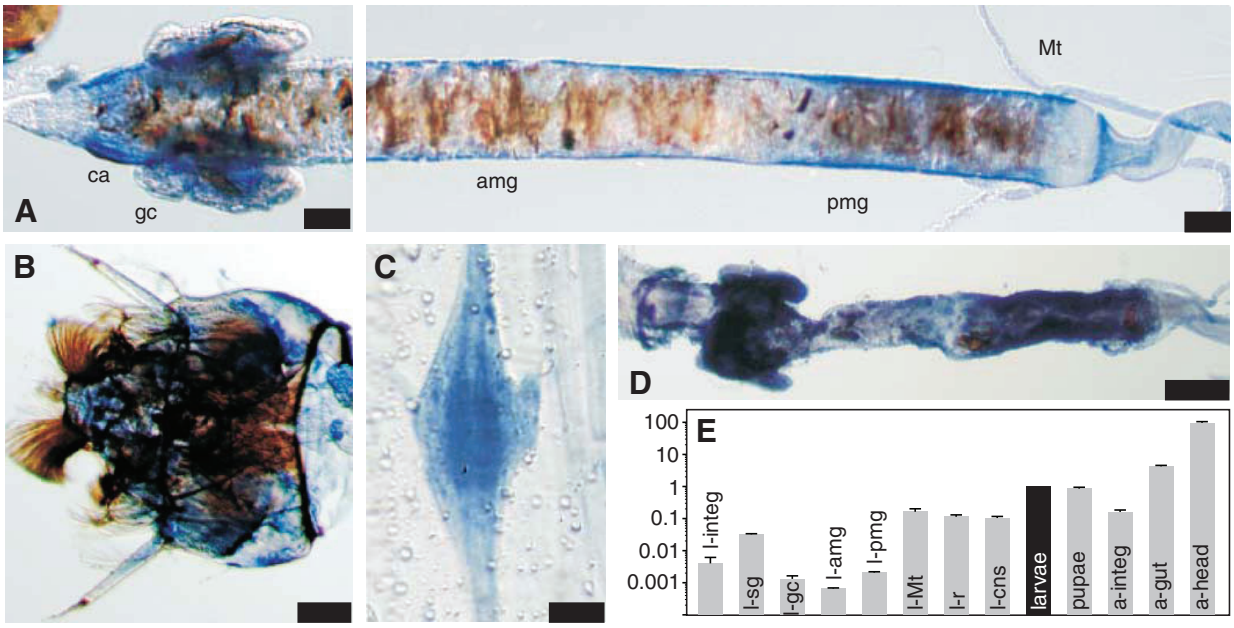

Fig. 5. AgNAT6 transcription in the alimentary canal and neuronal system of mosquito larvae. (A) *In situ* hybridization of AgNAT6 in the anterior and posterior portions of the whole-mount gut of 4th instar larvae. (B) Pattern of AgNAT6 hybridization in the larval head. (C) Strong hybridization signal in the neuropile of a larval abdominal ganglion. (D) More intense hybridization was detected in the gut from earlier 3rd instar larvae. The blue color represents the intensity of the hybridization signal. Scale bars are 200 μm. (E) Result of quantitative PCR assay of AgNAT6 transcript across different tissues and developmental stages of *An. gambiae* (data were normalized relative to values in whole larvae represented by the black bar; bars are means ± s.d.; *N*=3 for each data point). Abbreviations: amg, anterior midgut; ca, cardia; gc, gastric caeca; pmg, posterior midgut, a putative nutrient amino acid absorption site; Mt, Malpighian tubules; sg, salivary glands; r, rectum; cns, central nervous system; l, larvae; a, adult. The l-sg samples also include heart; a-integ samples include the ventral nerve cord and a-gut samples include the reproductive organs. Vertical scale is a log of relative transcript density.

specific and K^+-preferring NATs such as mammalian B^0ATs (Broer et al., 2004; Broer et al., 2006) and caterpillar KAAT1 (Castagna et al., 1998), reflecting adaptations of these organisms to high-sodium ion (in mammals) and trace-sodium ion/high-potassium ion (in caterpillars) environments. Correspondingly, the capacity of AgNATs to use Na^+ and K^+ can be explained as an adaptation to varied concentrations of these cations. For example, mosquito larvae are able to deal with low concentrations of both alkali metal cations in their freshwater habitat. A cation pool that is depleted by NATs activity in the absorptive region of the posterior midgut may be internally recycled in mosquito larvae *via* the earlier proposed anterior midgut alkalinization pathways (Harvey et al., 2009; Okech et al., 2008a). However, considering the limited efficiency of a cation-recycling framework, the balance of the Na^+/K^+ flux would be dependent upon the environmental availability of these ions. The availability of Na^+ and K^+ also varies over the life history of adult mosquitoes. The use of Na^+ is expected to be very low in adults feeding on plant fluids; but it may increase dramatically after a blood meal.

Both aromatic NATs are sensitive to extracellular Cl^- activity. When it is present outside Cl^- increases the net current that is carried *via* these transporters (Fig. 3D,E). This observation suggests that

Table 2. Aromatic amino acid transporters

MTS, type	SLC (HUGO)	Name	Mechanism*	Preferred substrates	References	***
B^{0+}	SLC6A14	$ATB^{0,+}$	s[AA][2Na^+Cl^-]	KRASCTNQHMILVFYW	Sloan and Mager, 1999	Sl
B^0	SLC6A19	B^0AT1	s[AA][Na^+]	ASCTQFWY	Broer et al., 2004	Sl
B^0 like		DmNAT1	s[AA][Na^+]	KRASCTNQHMILVFYW	Miller et al., 2008	Sl
B^0 like		AgNAT8	s[AA][2Na^+/K^+]	FY(L-DOPA)	Meleshkevitch et al., 2006	
B^0 like		AgNAT6	s[AA][2/1Na^+/K^+]	WY(5-HTP)	This study	
L	SLC7A5	LAT1	e[AA]:[AA]**	ASCTQFWY	Mastroberardino et al., 1998	Sl
y+	SLC7A8	LAT2	e[AA]:[AA]**	QHMLIVFYW	Broer et al., 2000	sl, bl
b^{0+}	SLC7A9	$b^{0,+}$AT	e[AA^+]:[AA^0]	KRASCTNQHMILVFYWC	Rajan et al., 1999	sl
b^{0+}	SLC7A15	arpAT	e[AA^+]:[AA^0]	KRASCTNQHMILVFYWC	Fernandez et al., 2005	sl
T	SLC16A10	TAT	u (passive flux)	FYW (low affinity)	Kim et al., 2001	bl, pf

*Mechanism abbreviations are: s, symporter, e, obligatory exchanger; u, uniporter or facilitated flux mechanism.

**Tertiary active uptake transporter for amino acids exchanged for intracellular amino acids, which were accumulated, for instance, *via* a metabolic pathway or Na^+-coupled symporter.

***Factors which limit or make impossible a contribution of the specified transporter in the accumulation of aromatic amino acids. Specific constrains are abbreviated as: sl, selectivity; bl, basolateral location in absorptive epithelia; pf, passive flux; la, insufficiently low affinity. Other abbreviations: AA, amino acid; MTS, mammalian transport system; SLC, solute carrier family; ref, representative references.

Cl^- may act as a NAT modulator rather than an electrophoretic carrier because adding negative charges to an inward cation:neutral amino acid symport will reduce rather than increase the net inward current (e.g. Fig. 3D; by convention in neurophysiology and insect epithelial transport physiology a positive ion moving into a cell or a negative ion moving out is said to carry an inward current). The data present another interesting possibility – that AgNAT6 function is facilitated by bidirectional (electroneutral) Cl^- transport. During outward movement Cl^- may energize changes in transporter conformation. A similar mechanism was described in SLC1 transporters that use K^+ to reset conformations (reviewed by Kanai and Hediger, 2004). The structural basis of Cl^- interaction with SLC6 members was the subject of a recent analysis suggesting a possible replacement of Cl^- by another negatively charged ion in chloride-independent members of SLC6 (Forrest et al., 2007; Zomot et al., 2007). However, the exact role of this anion in SLC6 function remains to be clarified. AgNAT6–Cl^- interaction will require a more detailed analysis that would be well beyond the scope of an initial characterization of AgNAT6.

Despite its obvious similarity with AgNAT8, the electrochemical properties of AgNAT6 have some unique traits. A most notable difference is in organic substrate specificity with AgNAT6's strong and narrow preference to indole-branched substrates (Fig. 3A, Fig. 4A,B). Collected data suggest that AgNAT6 is specialized to transport tryptophan with minimal interference from phenylalanine and other neutral amino acids, the cumulative concentration of which is about two orders of magnitude greater than that of tryptophan in the larval and adult nutrient digests [inferred from the frequency of amino acids in protein sequences (Brooks et al., 2002)]. Comparison of AgNAT6 and AgNAT8 (Meleshkevitch et al., 2006) *in situ* hybridization (Fig. 5) and immunolabeling (Okech et al., 2008b) profiles revealed broadly similar localizations, but with notable differences in the details. Specifically, AgNAT6 occupies a broader area of the larval gut (Fig. 5) with significant differences in the polar distribution in the gastric caeca and anterior midgut area relative to AgNAT8 (Okech et al., 2008b). Aromatic AgNATs also possess different expression patterns in the central nervous system and sensory afferents (Fig. 5B,C) (Meleshkevitch et al., 2006). These differences in expression may both reduce morphological overlap of aromatic NATs activities and support specific functions with elevated requirements for aromatic substrates. In the midgut the differing distributions may reduce competition of aromatic AgNATs for the energy of transmembrane electrochemical gradients whereas in the CNS they may support cell-specific metabolic processes, e.g. synthesis of indoleamine and catecholamine neurotransmitters.

AgNAT6 generates a large Na^+ leak current that was not observed upon heterologous expression of AgNAT8 (Meleshkevitch et al., 2006) or any other mosquito NAT such as AeAAT1 from *Aedes aegypti* (Boudko et al., 2005a). In this respect AgNAT6 is similar to CAATCH1 from the caterpillar (Quick and Stevens, 2001), which may act as a cationic leak channel with some inhibition by weakly transported substrates (i.e. Fig. 3C for L-Phe and L-DOPA). However, that kind of response was observed only 6–8 days after injection of AgNAT6 RNA into oocytes. It equally may be an artifact of heterologous over-expression rather than a physiologically significant mechanism. Additional experiments will be necessary to validate this phenomenon and to understand its physiological implications.

The pH dependency profile of AgNAT6 is different from that of AgNAT8, perhaps reflecting adaptations to the changing pH profile along the alimentary canal of mosquito larvae (Clements, 1992; Ramsay, 1950). The transport stoichiometry of AgNAT6 changes reversibly between 1 and 2 Na^+ per amino acid transported. The physiological benefit of such an adaptation is obvious: 1:1 operation will conserve Na^+ pool-coupled electrochemical energy, whereas 1:2 operation permits organic substrate translocation against a 2 times higher chemical gradient. The recent crystallographic structure of the bacterial NAT-SLC6 member $LeuT_{Aa}$ suggests that a single sodium ion is sufficient for substrate coordination in the substrate-binding pocket of the transporter (Yamashita et al., 2005). The paralogous mammalian B^0ATs operate with 1:1 substrate stoichiometry (Broer, 2008), whereas other members of the NTT-SLC6 subfamily may use 3, 2 or 1 Na^+ for 1 neurotransmitter molecule (Chen et al., 2004). For example, GlyT2a and GlyT1b expressed in neuronal and glial cells respectively conduct $3\,Na^+$:Cl^-:Gly and $2\,Na^+$:Cl^-:Gly symport (Roux and Supplisson, 2000). So, switching of a 'stoichiometry gear' – often referred to as a 'slip' – is common in the history of SLC6 family members, even among recently diverged transporters. It is also likely that the slip in AgNAT6 stoichiometry may depend upon physiological conditions *via* a yet to be elucidated mechanism. Incidentally, the 'low' tested concentration of the substrate is still 230-fold greater than that of the $K_{50}{}^{Trp}$, suggesting an organic substrate binding, kinetically uncoupled mechanism. Considering the possibility of a concentration-dependent shift of the dose–response curve, a more direct and precise technique of stoichiometry assays will be necessary to clarify this phenomenon.

The presently characterized aromatic amino acid-specific NATs include one bacterial (Androutsellis-Theotokis et al., 2003) and two mosquito transporters (Meleshkevitch et al., 2006; Okech et al., 2008b) (and data presented here). The usage of aromatic amino acids varies dramatically in different organisms, developmental stages, tissues and individual cells. Their availability also varies with ecological and nutrient conditions. For example, freshwater mosquito larvae filter-feeding on micro-organisms and organic debris, and mammals digesting protein-rich food may have a different concentration profile of essential amino acids in the alimentary canal and systemic circulations. Mosquito larvae require high quantities of aromatic amino acids for cuticle formation and tanning during successive ecdyses as well as protein accumulation between ecdysial events. A high-throughput transport of aromatic amino acids from the digestive system to the ovaries is critical during egg development and chorion formation. AgNAT6 is perfectly suited to acquire the most under-represented essential amino acids from the larval environment as well as to normalize the supply of such amino acids during specific metabolic processes such as oogenesis or neurotransmitter synthesis.

In summary, we have characterized the first eukaryotic Na^+:tryptophan symporter, AgNAT6, which also represents the second characterized narrow substrate spectra transporter (the first being AgNAT8) cloned from a biomedically important model organism, the African malaria mosquito, *An. gambiae*. AgNAT6 plays a key role in the uphill delivery of essential tryptophan and, in synergy with phenyl-branched substrate-specific AgNAT8, mediates comprehensive absorption and systemic redistribution of aromatic substrates. These narrow selectivity NATs may have evolved under pressure of high demand *vs* low availability for aromatic amino acids. A likely reason for the additional expansion of NATs in invertebrates with narrow substrate spectra is the amplification of the transport network for the acquisition and redistribution of environmentally scarce substrates. It is reasonable to propose that metazoan organisms competing for an identical set of essential amino acids evolved distinct strategies and mechanisms for their absorption and redistribution. Future analysis of NAT

populations is necessary for a better understanding of the structural, integrative and evolutionary aspects of SLC6 functions. The fact that NATs are lineage-specific and unique providers of essential for development substrates identifies them as targets for environmentally safe control of pests and pathogen-transmitting invertebrate organisms.

This work was supported in part by NIH/NIAID grant R01 AI-030464 and the Whitney Laboratory for Marine Bioscience (P. A. V. Anderson, director). Deposited in PMC for release after 12 months.

REFERENCES

Androutsellis-Theotokis, A., Goldberg, N. R., Ueda, K., Beppu, T., Beckman, M. L., Das, S., Javitch, J. A. and Rudnick, G. (2003). Characterization of a functional bacterial homologue of sodium-dependent neurotransmitter transporters. *J. Biol. Chem.* **278**, 12703-12709.

Boudko, D. Y., Kohn, A. B., Meleshkevitch, E. A., Dasher, M. K., Seron, T. J., Stevens, B. R. and Harvey, W. R. (2005a). Ancestry and progeny of nutrient amino acid transporters. *Proc. Natl. Acad. Sci. USA* **102**, 1360-1365.

Boudko, D. Y., Stevens, B. R., Donly, B. C. and Harvey, W. R. (2005b). Nutrient amino acid and neurotransmitter transporters. In *Comprehensive Molecular Insect Science*, vol. 4 (ed. K. Iatrou, S. S. Gill and L. I. Gilbert), pp. 255-309. Amsterdam: Elsevier.

Broer, A., Wagner, C. A., Lang, F. and Broer, S. (2000). The heterodimeric amino acid transporter 4F2hc/y(+)LAT2 mediates arginine efflux in exchange with glutamine. *Biochem. J.* **349**, 787-795.

Broer, A., Klingel, K., Kowalczuk, S., Rasko, J. E. J., Cavanaugh, J. and Broer, S. (2004). Molecular cloning of mouse amino acid transport system B-0, a neutral amino acid transporter related to Hartnup disorder. *J. Biol. Chem.* **279**, 24467-24476.

Broer, A., Tietze, N., Kowalczuk, S., Chubb, S., Munzinger, M., Bak, L. K. and Broer, S. (2006). The orphan transporter v7-3 (slc6a15) is a Na+-dependent neutral amino acid transporter (B0AT2). *Biochem. J.* **393**, 421-430.

Broer, S. (2008). Amino acid transport across mammalian intestinal and renal epithelia. *Physiol. Rev.* **88**, 249-286.

Brooks, D. J., Fresco, J. R., Lesk, A. M. and Singh, M. (2002). Evolution of amino acid frequencies in proteins over deep time: inferred order of introduction of amino acids into the genetic code. *Mol. Biol. Evol.* **19**, 1645-1655.

Castagna, M., Shayakul, C., Trotti, D., Sacchi, V. F., Harvey, W. R. and Hediger, M. A. (1998). Cloning and characterization of a potassium-coupled amino acid transporter. *Proc. Natl. Acad. Sci. USA* **95**, 5395-5400.

Chakrabarti, A. C. (1994). Permeability of membranes to amino acids and modified amino acids: mechanisms involved in translocation. *Amino Acids* **6**, 213-229.

Chakrabarti, A. C. and Deamer, D. W. (1994). Permeation of membranes by the neutral form of amino acids and peptides: relevance to the origin of peptide translocation. *J. Mol. Evol.* **39**, 1-5.

Chen, N. H., Reith, M. E. and Quick, M. W. (2004). Synaptic uptake and beyond: the sodium- and chloride-dependent neurotransmitter transporter family SLC6. *Pflugers Arch.* **447**, 519-531.

Clements, A. N. (1992). *The Biology of Mosquitoes*. London: Chapman & Hall.

Felsenstein, J. (1985). Confidence limits on phylogenies: an approach using the bootstrap. *Evolution* **39**, 783-791.

Fernandez, E., Torrents, D., Zorzano, A., Palacin, M. and Chillaron, J. (2005). Identification and functional characterization of a novel low affinity aromatic-preferring amino acid transporter (arpAT). One of the few proteins silenced during primate evolution. *J. Biol. Chem.* **280**, 19364-19372.

Forrest, L. R., Tavoulari, S., Zhang, Y. W., Rudnick, G. and Honig, B. (2007). Identification of a chloride ion binding site in Na+/Cl-dependent transporters. *Proc. Natl. Acad. Sci. USA* **104**, 12761-12766.

Harvey, W. R., Boudko, D. Y., Rheault, M. R. and Okech, B. A. (2009). NHEVNAT: an H+ V-ATPase electrically coupled to a Na+:nutrient amino acid transporter (NAT) forms an Na+/H+ exchanger (NHE). *J. Exp. Biol.* **212**, 347-357.

Holt, R. A., Subramanian, G. M., Halpern, A., Sutton, G. G., Charlab, R., Nusskern, D. R., Wincker, P., Clark, A. G., Ribeiro, J. M., Wides, R. et al. (2002). The genome sequence of the malaria mosquito Anopheles gambiae. *Science* **298**, 129-149.

Jespersen, T., Grunnet, M., Angelo, K., Klaerke, D. A. and Olesen, S. P. (2002). Dual-function vector for protein expression in both mammalian cells and Xenopus laevis oocytes. *Biotechniques* **32**, 536-538.

Kanai, Y. and Hediger, M. A. (2004). The glutamate/neutral amino acid transporter family SLC1: molecular, physiological and pharmacological aspects. *Pflugers Arch.* **447**, 469-479.

Kim, D. K., Kanai, Y., Chairoungdua, A., Matsuo, H., Cha, S. H. and Endou, H. (2001). Expression cloning of a Na+-independent aromatic amino acid transporter with structural similarity to H+/monocarboxylate transporters. *J. Biol. Chem* **276**, 17221-17228.

Marti-Renom, M. A., Stuart, A. C., Fiser, A., Sanchez, R., Melo, F. and Sali, A. (2000). Comparative protein structure modeling of genes and genomes. *Annu. Rev. Biophys. Biomol. Struct.* **29**, 291-325.

Mastroberardino, L., Spindler, B., Pfeiffer, R., Skelly, P. J., Loffing, J., Shoemaker, C. B. and Verrey, F. (1998). Amino-acid transport by heterodimers of 4F2hc/CD98 and members of a permease family. *Nature* **395**, 288-291.

Meleshkevitch, E. A., Assis-Nascimento, P., Popova, L. B., Miller, M. M., Kohn, A. B., Phung, E. N., Mandal, A., Harvey, W. R. and Boudko, D. Y. (2006). Molecular characterization of the first aromatic nutrient transporter from the sodium neurotransmitter symporter family. *J. Exp. Biol.* **209**, 3183-3198.

Miller, M. M., Popova, L. B., Meleshkevitch, E. A., Tran, P. V. and Boudko, D. Y. (2008). The invertebrate B(0) system transporter, D. melanogaster NAT1, has unique d-amino acid affinity and mediates gut and brain functions. *Insect Biochem. Mol. Biol.* **38**, 923-931.

Nicholas, K. B., Nicholas, H. B., Jr and Deerfield, D. W., II (1997). GeneDoc: analysis and visualization of genetic variation. *EMBNET News* **4**, 14.

Okech, B. A., Boudko, D. Y., Linser, P. J. and Harvey, W. R. (2008a). Cationic pathway of pH regulation in larvae of *Anopheles gambiae*. *J. Exp. Biol.* **211**, 957-968.

Okech, B. A., Meleshkevitch, E. A., Miller, M. M., Popova, L. B., Harvey, W. R. and Boudko, D. Y. (2008b). Synergy and specificity of two Na+-aromatic amino acid symporters in the model alimentary canal of mosquito larvae. *J. Exp. Biol.* **211**, 1594-1602.

Quick, M. and Stevens, B. R. (2001). Amino acid transporter CAATCH1 is also an amino acid-gated cation channel. *J. Biol. Chem.* **276**, 33413-33418.

Rajan, D. P., Kekuda, R., Huang, W., Wang, H., Devoe, L. D., Leibach, F. H., Prasad, P. D. and Ganapathy, V. (1999). Cloning and expression of a b(0,+)-like amino acid transporter functioning as a heterodimer with 4F2hc instead of rBAT. A new candidate gene for cystinuria. *J. Biol. Chem.* **274**, 29005-29010.

Ramsay, J. A. (1950). Osmotic regulation in mosquito larvae. *J. Exp. Biol.* **27**, 145-157.

Roux, M. J. and Supplisson, S. (2000). Neuronal and glial glycine transporters have different stoichiometries. *Neuron* **25**, 373-383.

Sali, A. and Blundell, T. L. (1993). Comparative protein modeling by satisfaction of spatial restraints. *J. Mol. Biol.* **234**, 779-815.

Sloan, J. L. and Mager, S. (1999). Cloning and functional expression of a human Na+ and Cl-dependent neutral and cationic amino acid transporter B0+. *J. Biol. Chem.* **274**, 23740-23745.

Sneath, P. H. A. and Sokal, R. R. (1973). *Numerical Taxonomy: The Principles and Practice of Numerical Classification*. San Francisco, CA: W. H. Freeman.

Tamura, K., Dudley, J., Nei, M. and Kumar, S. (2007). MEGA4: Molecular Evolutionary Genetics Analysis (MEGA) software version 4.0. *Mol. Biol. Evol.* **24**, 1596-1599.

Thompson, J. D., Gibson, T. J., Plewniak, F., Jeanmougin, F. and Higgins, D. G. (1997). The CLUSTAL_X windows interface: flexible strategies for multiple sequence alignment aided by quality analysis tools. *Nucleic Acids Res.* **25**, 4876-4882.

Ueda, K., Yamashita, A., Ishikawa, J., Shimada, M., Watsuji, T. O., Morimura, K., Ikeda, H., Hattori, M. and Beppu, T. (2004). Genome sequence of Symbiobacterium thermophilum, an uncultivable bacterium that depends on microbial commensalism. *Nucleic Acids Res.* **32**, 4937-4944.

Yamashita, A., Singh, S. K., Kawate, T., Jin, Y. and Gouaux, E. (2005). Crystal structure of a bacterial homologue of Na+/Cl-dependent neurotransmitter transporters. *Nature* **437**, 215-223.

Zomot, E., Bendahan, A., Quick, M., Zhao, Y., Javitch, J. A. and Kanner, B. I. (2007). Mechanism of chloride interaction with neurotransmitter:sodium symporters. *Nature* **449**, 726-730.

Zuckerkandl, E. and Pauling, L. (1965). *Evolutionary Divergence and Convergence in Proteins*. New York: Academic Press.